On the use of water vapour radiometry for assessment of wet delay estimates from space geodetic techniques

On the use of water vapour radiometry for assessment of wet delay estimates from space geodetic techniques

G. Elgered, T. Ning

Abstract We have studied the impact of liquid water drops in the atmosphere on the retrieval accuracy of the wet propagation delay using microwave radiometry through a comparison with the corresponding results from ground-based GPS observations. Using all data available acquired at the Onsala Space Observatory during 2022 we find, as expected, the best agreement for the conditions with no, or a very small, liquid water content (LWC). For the LWC interval 0.0–0.1 mm the bias and the standard deviation of the equivalent zenith wet delay (ZWD) agreement between the WVR and the GPS estimates are 3.3 mm and 4.2 mm, respectively.

Keywords microwave radiometry, wet delay, GPS

Fig. 1 The GNSS station ONSA (left, at the end of the cable tray) and the Water Vapour Radiometer (WVR) Konrad (in the foreground). The twin telescopes, and the 25 m radio telescope, are seen in the background. A new WVR (to the right), manufactured by RPG, was installed in May 2023, but has not been used in this study.

1 Introduction

During the development of the Mark III VLBI system in the seventies, water vapour radiometers (WVR) were envisaged to provide independent observations of the signal propagation delay due to water vapour along the line of sight. The standard design of the WVR is to measure the atmospheric emission at two frequencies, close to and further away from the centre of the water vapour emission line at 22.2 GHz (Wu, 1979). These measurements are used to estimate two unknowns, the amount of water vapour, or the wet delay, and the liquid water content (LWC) along the line of sight.

We have assessed the retrieval accuracy of the equivalent zenith wet delay (ZWD) from WVR data and its dependence on the estimated LWC by comparing them to those estimated from data acquired by the GNSS station ONSA. Fig. 1 depicts the ONSA station and the WVR Konrad.

The main drawback of using a WVR is that the retrieval algorithm requires that any liquid water drops in the sensed volume of air are much smaller than the wavelength observed by the WVR, i.e., ≈ 1 cm (Westwater & Guiraud, 1980). Therefore, the algorithm more or less breaks down during rain, meaning that the WVR cannot be relied on for 100 % of time, unless it never rains on, or close to, the site. The method generally used is to avoid using WVR data with poor accuracy by ignoring observations obtained during rain and when the inferred equivalent zenith LWC is above a specific

Gunnar Elgered
Chalmers University of Technology, Onsala Space Observatory, SE-439 92 Onsala, Sweden

Tong Ning
Lantmäteriet (Swedish Mapping, Cadastral and Land Registration Authority), SE-801 82 Gävle, Sweden

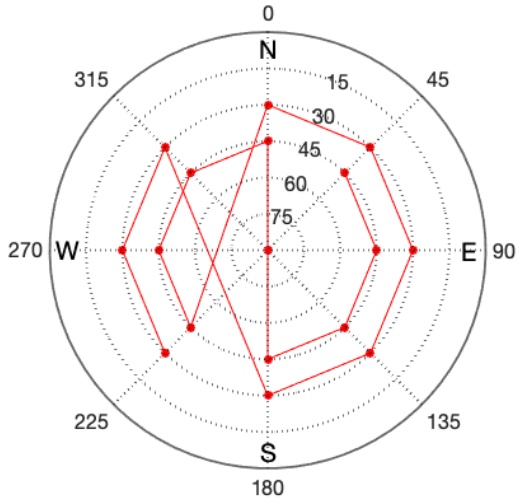

Fig. 2 The observational cycle of the Konrad WVR.

threshold. This method is, however, subject to some uncertainties: (i) There may be rain drops in the sensed volume of air in spite of the fact that no drops are detected at the ground on the site; (ii) there may still be drops of water on the WVR instrument many minutes after the rain has stopped, such as on the protective covers of the horn antennas and on the mirrors; and (iii) a low density of large drops may result in a smaller liquid water content than many small drops.

2 Data

The WVR observes the thermal emission from the sky in two different frequency channels: 20.64 GHz and 31.60 GHz. Each channel has a double sideband mixer and a total RF bandwidth of 320 MHz.

The WVR was operated continuously from mid-January to the end of 2022. The data were acquired using the same procedure mapping the sky. The observations were distributed on the sky covering the full range of azimuth angles at elevation angles above 30°. The different observational directions are illustrated in Fig. 2. These 17 samples took approximately 2 min and this cycle was repeated continuously.

Periods with rain and all individual observations resulting in an equivalent zenith LWC larger than 0.7 mm were deleted. Thereafter, for each 5 min period, having more than 30 observations, the equivalent zenith wet delay (ZWD), its time derivative, and the linear horizontal gradients in the east and in the north directions were estimated using the four parameter model described by Davis et al. (1993). This resulted in 78,814 data points, corresponding to a time coverage of 75 % of the year. After synchronising with the available GPS data, there were 77,972 data points.

The GNSS data were processed with the GipsyX software, using satellites in the GPS constellation and an elevation cutoff angle of 10°. The ZWD and the east and the north horizontal gradients were estimated every 5 min, with constraints equal to 10 mm/$\sqrt{\mathrm{h}}$ and 0.3 mm/$\sqrt{\mathrm{h}}$, respectively.

For more details about the WVR specifications and the GPS data processing, see Elgered et al. (2023).

3 Results

The ZWD estimates for the ONSA GPS data are shown together with the ZWD differences between the WVR and the GPS in Fig. 3. The ZWD differences shown in Fig. 3 are also shown in Fig. 4 but here vs. the LWC. The seasonal dependence and the large variability in the ZWD is clear and well known. It can also be noted that because first all individual observations with an LWC larger than 0.7 mm are ignored and, thereafter, an average is calculated for each 5 min period, the number of data points in Fig. 4 with an LWC larger than say 0.5 mm becomes relatively small. This would of course change if the temporal resolution is higher, but in this study we are limited by the 5 min temporal resolution for the GPS estimates.

For a large LWC we note a positive bias (WVR−GPS) for the ZWD. In Fig. 4 we also include a small negative LWC (LWC $>$ −0.05 mm) in order to allow for some noise in the sky brightness temperatures. However, observations implying a negative LWC will also introduce a positive bias in the ZWD because it indicates that we have either a positive error in 20.64 GHz channel, or a negative error in the 31.60 GHz channel, or a combination of these.

In June, July, and August there are a few occasions with large negative differences (see Fig. 3). Most of these are associated with a large and rapid change in the ZWD and a time delay between the WVR and the GPS. We assume that the WVR ZWD are more correct because of the constraint used in the estimation pro-

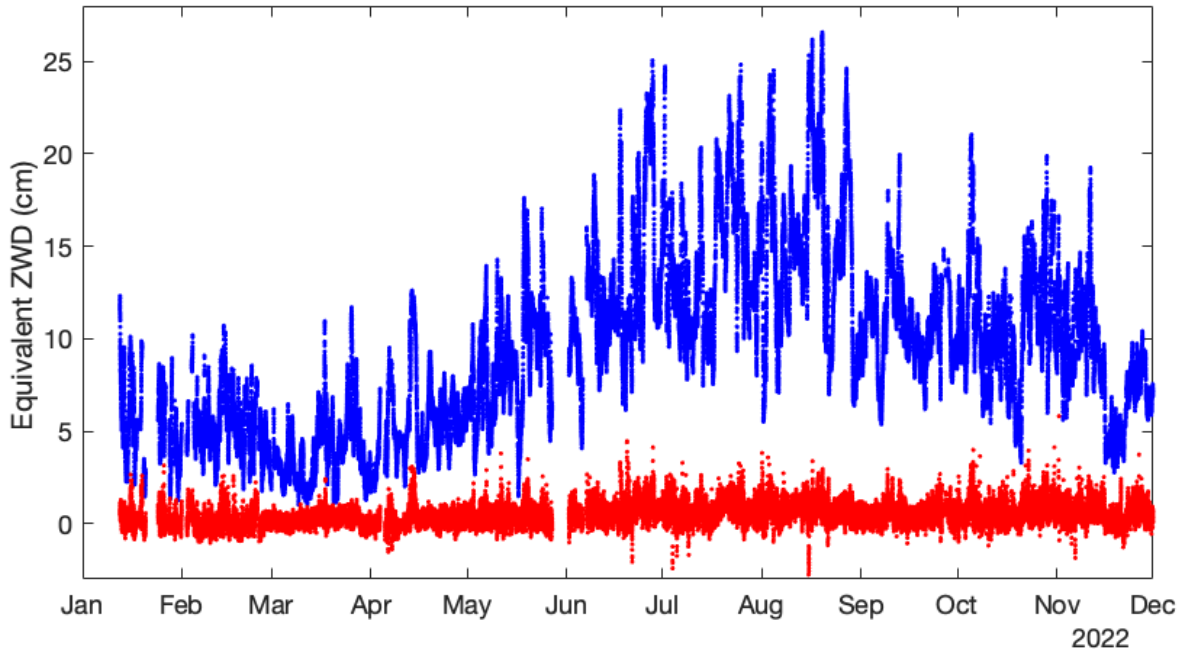

Fig. 3 ZWD using GPS data from ONSA (blue dots) and the ZWD difference WVR–GPS (red dots). The data are synchronized and most data gaps are periods of rain and LWC vaues larger than 0.7 mm. One exception is in the beginning of May when WVR data were lost due to a local network failure.

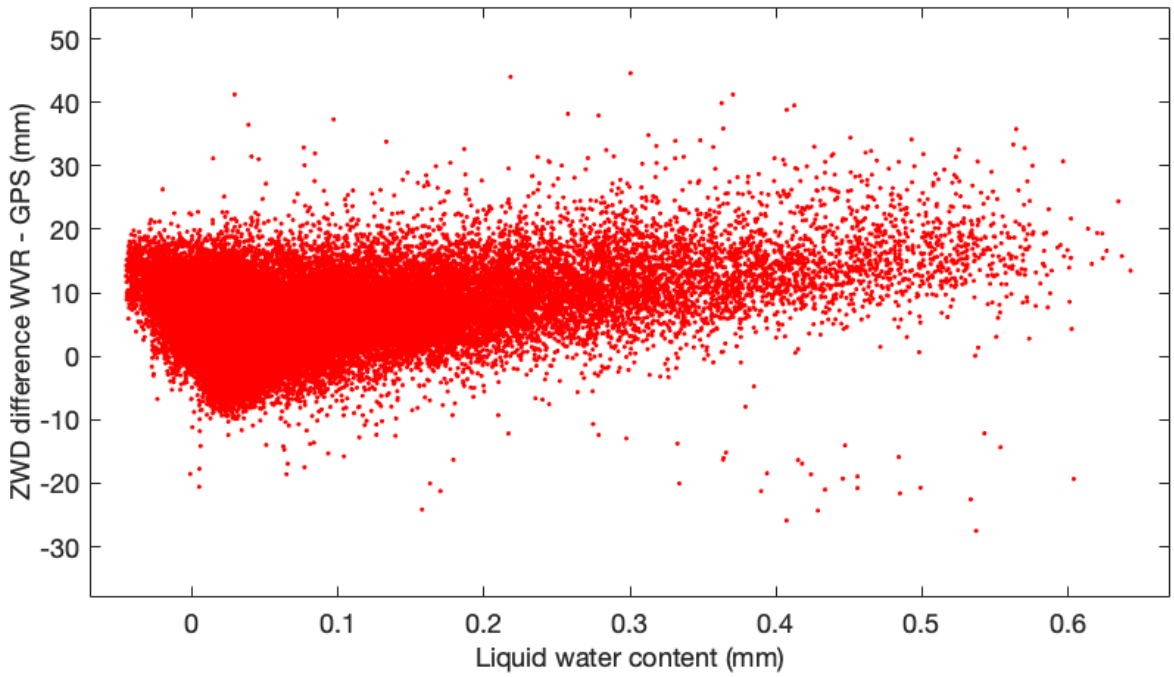

Fig. 4 Equivalent ZWD differences: WVR–GPS. The small amount of data for high LWC is is a bit misleading. The reason is that the graph contains 5 min averages that were calculated after that all individual LWC values larger than 0.7 mm in the equivalent zenith direction were removed.

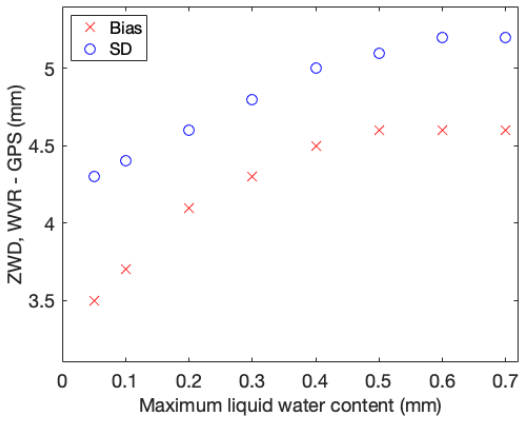

Fig. 5 The bias and the SD for the WVR–GPS differences of the ZWD vs the maximum LWC for the data used, inferred from the WVR observations. The number of data points is reduced from 77,966 for LWC < 0.7 mm to 56,176 for LWC < 0.05 mm.

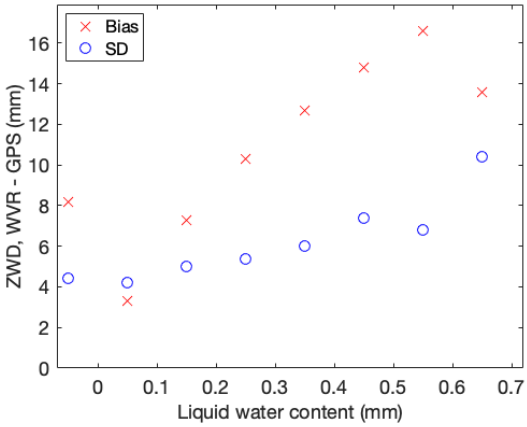

Fig. 7 The bias and the SD for the WVR–GPS differences of the ZWD for different intervals of the inferred LWC from WVR observations. Note the different scale compared to Fig. 5. The values are also presented in Table 1.

cess of the GPS data, whereas adjacent values in the WVR time series are independent. On 15 August the large differences are caused by unexplained high sky temperatures observed by the 31.4 GHz channel.

We investigate how the bias and the standard deviation (SD) of the ZWD and the gradients depend on the allowed LWC. Two different approaches are used to illustrate the dependence. Figs. 5 and 6 illustrate how the WVR ZWD and the gradients are improved compared to the GPS results when the maximum LWC is reduced. The minimum LWC is at -0.05 mm in all cases. The second approach is motivated because the number of data points are very different in the different LWC intervals. In this case we calculate the bias and the SD for different LWC intervals. These results are illustrated for the ZWD and the gradients in Fig. 7 and Fig. 8, respectively. The specific values are also presented in Table 1.

The improvement is larger for the ZWD compared to the gradients when the maximum LWC is reduced. The small improvement for the gradients is because the differences are dominated by the different sampling of the sky for the WVR and the GPS.

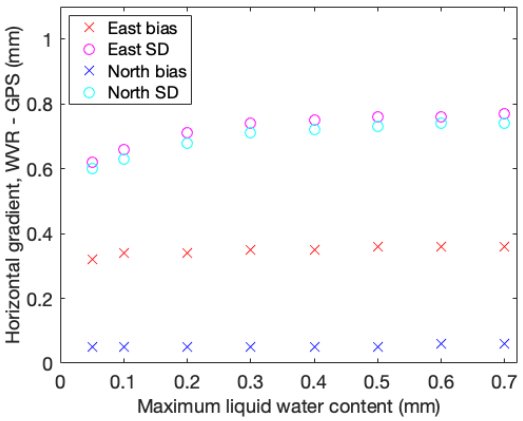

Fig. 6 The bias and the SD for the WVR–GPS differences of the linear horizontal gradients vs the maximum LWC for the data used, inferred from the WVR observations. The number of data points are the same as in Fig. 5

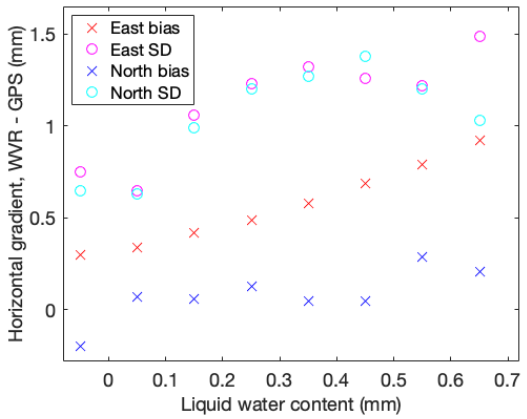

Fig. 8 The bias and the SD for the WVR–GPS differences of the linear horizontal gradients for different intervals of the inferred LWC from WVR observations. Note the different scale compared to Fig. 6. The values are also presented in Table 1.

Table 1 ZWD and horizontal gradient comparison between the Konrad WVR and GPS estimates

Interval of LWC	No. of data points	Relative amount of all data	ZWD		Horizontal gradient			
					East		North	
(mm)		(%)	Bias (mm)	SD (mm)	Bias (mm)	SD (mm)	Bias (mm)	SD (mm)
−0.05–0.0	4 979	6.39	8.2	4.4	0.30	0.75	−0.20	0.65
0.0–0.1	59 990	76.96	3.3	4.2	0.34	0.65	0.07	0.63
0.1–0.2	7 363	9.45	7.3	5.0	0.42	1.06	0.06	0.99
0.2–0.3	3 065	3.93	10.3	5.4	0.49	1.23	0.13	1.20
0.3–0.4	1 477	1.89	12.7	6.0	0.58	1.32	0.05	1.27
0.4–0.5	752	0.96	14.8	7.4	0.69	1.26	0.05	1.38
0.5–0.6	312	0.40	16.6	6.8	0.79	1.22	0.29	1.20
0.6–0.7	14	0.02	13.6	10.4	0.92	1.49	0.21	1.03

In the ZWD graphs (Figs. 5 and 7) it is clear that both the bias and the SD increase with increasing LWC. Note that the values for the two intervals with the highest LWC (Fig. 7) are more uncertain because of the low amount of data points. The increasing bias seen for the ZWD estimates confirm earlier results that the WVR tends to overestimate the ZWD when the LWC is increasing (Elgered et al., 1991).

For the gradients (Figs. 6 and 8) the SD also increase with an increasing LWC. This is expected since more liquid water clouds imply a less homogeneous atmosphere and the different sampling directions will have a greater impact. We do not expect that the bias in the gradients will increase with the LWC. However, we do see such a trend for the east gradient. We can speculate that because the WVR in general overestimates the wet delay for high LWC, and given that the location is at the coastline, oriented roughly in the south-north direction, more clouds with a higher LWC over land compared to over the sea could be the cause. More work is, however, needed in order to confirm such an explanation.

4 Conclusions and outlook

Using WVR data for validation of ZWD estimates in space geodesy means that data must not necessarily be available for all time periods. We can ignore more or less data with a high LWC, meaning that there is a balance between how much data we want to have available and the data accuracy.

As a consequence, a future application, for time periods when no liquid water is present in the atmosphere, would be to develop a one-frequency radiometer with high stability and accuracy.

References

Davis J L, Elgered G, Niell A E, and Kuehn C E (1993), Ground-based measurement of gradients in the "wet" radio refractive index of air, Radio Sci., 28(6), 1003–1018. https://doi.org/10.1029/93RS01917

Elgered, G. Davis J L, Herring T A, Shapiro I I (1991), Geodesy by radio interferometry: water vapor radiometry for estimation of the wet delay, J. Geophys. Res., 96, 6541–6555. https://doi.org/10.1029/90JB00834

Elgered G, Ning T, Diamantidis P K, Nilsson T (2023). Assessment of GNSS stations using atmospheric horizontal gradients and microwave radiometry, Adv. Space Res. https://doi.org/10.1016/j.asr.2023.05.010

Westwater E R, Guiraud F O, (1980). Ground-based microwave radiometric retrieval of precipitable water vapor in presence of clouds with high liquid content. Radio Sci., 15, 947–957. https://doi.org/10.1029/RS015i005p00947

Wu S C (1979). Optimum frequencies of a passive microwave radiometer for tropospheric path-length correction, *IEEE Trans. Ant. Propagat., AP-27, pp. 233–239*, *https://doi.org/10.1109/TAP.1979.1142066*.